Desalination and Water Treatment
www.deswater.com
doi: 10.1080/19443994.2015.1029530

57 (2016) 9510–9519
April

Taylor & Francis
Taylor & Francis Group

Facile synthesis of three-dimensional graphene–soy protein aerogel composites for tetracycline adsorption

Yuan Zhuang[a], Fei Yu[c], Jie Ma[a,*], Junhong Chen[a,b]

[a]*State Key Laboratory of Pollution Control and Resource Reuse, School of Environmental Science and Engineering, Tongji University, 1239 Siping Road, Shanghai 200092, P.R. China, Tel. +86 21 65981629; email: 527970764@qq.com (Y. Zhuang), Tel. +86 21 65981831; email: jma@tongji.edu.cn (J. Ma), Tel. +86 21 65981629; email: jhchen@tongji.edu.cn (J. Chen)*
[b]*Department of Mechanical Engineering, University of Wisconsin–Milwaukee, Milwaukee, WI 53211, USA*
[c]*College of Chemistry and Environmental Engineering, Shanghai Institute of Technology, Shanghai 2001418, P.R. China, Tel. +86 21 60873182; email: fyu@vip.163.com*

Received 30 August 2014; Accepted 7 March 2015

ABSTRACT

A three-dimensional graphene–soy protein aerogel was prepared and characterized by scanning electron microscopy, Raman, and fourier transform infrared spectroscopy. Both the graphene aerogel (GS0) and the graphene–soy protein aerogel (GS6) were used as adsorbents for the removal of tetracycline from an aqueous solution. The kinetics model (pseudo-first-order, pseudo-second-order, and intraparticle diffusion model), isotherm model (Langmuir, Freundlich, Temkin, and Dubinin–Radushkevich), and pH influences were investigated to characterize the adsorption behaviors. The Langmuir and the pseudo-second-order were best fitted for both GS0 and GS6. Calculated from the Langmuir model, the maximum adsorption capacity of GS0 was 137.0 mg/g, while GS6 was 164.0 mg/g. Graphene was decorated by low-cost and nontoxic protein with enhanced adsorption performance and low biotoxictiy. Therefore, GS6 is a promising adsorbent material for the preconcentration and separation of antibiotics for environmental remediation.

Keywords: Graphene; Protein; Aerogel; Adsorption

1. Introduction

Antibiotics are widely used around the world in medical care and the farming industry. However, they have received increasing attention in recent years because they are toxic to living beings. Exposures to residues of antibiotics and their transformed products might cause a variety of adverse effects, including acute and chronic toxicity, and micro-organism antibiotic resistance [1]. Hence, there is an increasing demand for the removal of antibiotics from water. Many kinds of antibiotics can be degraded biotically or abiotically in soils and water, which will reduce their potency; however, some degradation products may have similar toxicity to their parent compound [2]. Thus, adsorption is an effective method to remove antibiotics. Through a comparative study, Ji et al. [3] found that microporous activated carbons exhibited much lower adsorption affinity for bulky tetracycline molecules mainly due to the molecular sieving effect. Moreover, as a special adsorbent for organic contaminants, carbon nanotubes can be engineered and

*Corresponding author.

1944-3994/1944-3986 © 2015 Balaban Desalination Publications. All rights reserved.

functionalized on purpose to enhance the adsorption selectivity specific to the target compound. The results of the present work indicate that the adsorption selectivity and efficiency can be improved through specific molecular-level interactions between organic contaminants and carbon nanotubes. Thus, carbon nanomaterial has great potential for applications in antibiotics adsorption.

In the past several years, a free-standing two-dimensional monolayer graphene with excellent mechanical, electrical, and thermal properties has caught global attention and has been adopted for various applications [3]. Also, with great specific surface area (2,630 m^2/g), graphene has been considered as an excellent adsorbent. With its delocalized π bonds, graphene can potentially adsorb organic contaminants, especially these with molecules containing π-electrons that can interact with a polarized graphene surface via π–π electron coupling or Van der Waals interactions [4,5]. For application as an adsorbent, using three-dimensional (3D) graphene makes adsorbent separation easier. Tiwari et al. [6] synthesized a 3D reduced graphene oxide-based hydrogel that showed an excellent dye removal rate for methylene blue (100%) and rhodamine B (97%) in an aqueous solution through strong Van der Waals and π–π interactions.

As graphene has low solubility, biocompatible hydrophilic polymer has been used to cover nanostructures to provide them with high dispersibility [7]. Developing hydrophilic and biocompatible 3D structures graphene composites with a large specific surface area and unique mesoporosity would expand their significance in the area of environmental applications [8]. By composition with polymers, graphene composites could have better hydrophily, biological compatibility, and lower cytotoxicity. Moreover, gels can be prepared in large scale by means of a facile gelation process in a short time. Therefore, it is reasonable to predict that the biopolymer-mediated graphite oxide (GO) gels may function as porous adsorbents with satisfactory adsorption capacity and limited toxicity for an application in wastewater treatment [9].

Zhao et al. [10] reported that a porous graphene oxide–chitosan aerogel could be used as a recyclable adsorbent for tetracycline removal. Xu et al. [11] reported a strategy for 3D self-assembly of graphene oxide sheets and DNA to form multifunctional hydrogels that possessed high mechanical strength, environmental stability, and dye-loading capacity. Cheng et al. [9] prepared three typical GO-biopolymer gels (bovine serum albumin, chitosan, and double-stranded DNA) for the first time and investigated the adsorption capabilities of dyes and heavy metals. The GO-biopolymer gels displayed an adsorption capacity as high as 1,100 mg/g for methylene blue dye and 1,350 mg/g for methyl violet dye, respectively.

Natural polymers such as vegetable proteins also have attracted considerable research activities because of their availability, biodegradability, renewable character, and various interesting functional properties. Among them, proteins extracted from vegetable seeds (soybean, pea, barley, wheat, rice, oat, sunflower) have been reported as having good emulsifying and foaming capacities, water solubility, amphiphilic, and film-forming properties [12]. However, there are few studies on the composition of these proteins with graphene especially to form aerogels.

In this paper, graphene–soy protein aerogel (GS) is prepared by a simple thermal reduction method and then is used as an adsorbent for the removal of tetracycline from aqueous solutions. The resulting GS possesses desirable excellent adsorption properties for the removal of tetracycline with significantly enhanced adsorption capacity (164 mg/g).

2. Experimental and computational methods

2.1. Materials

All chemicals were purchased from Sinopharm Chemical Reagent Co., Ltd (Shanghai, China) in analytical purity and used in the experiments directly without any further purification. All solutions were prepared using deionized water.

2.2. Preparation of graphene–soy protein aerogels

GO was obtained by Hummers methods [13], which was dispersed in deionized water and sonicated in an ultrasound bath for 12 h. Soy protein and ascorbic acid were added into the GO solution and put into an ultrasound bath for 5 h to form a uniform solution. The mass ratio of graphene to soy protein varied at 1:0, 1:2, 1:4, 1:6, 1:8, 1:10 and the resulting aerogels were denoted as GS0, GS2, GS4, GS6, GS8, GS10, respectively. The mixture was heated in a water bath under 90°C for 12 h to form hydrogels. After the hydrogels were washed several times by distilled water, and freeze-dried for 24 h, aerogels were synthesized.

2.3. Characterization methods

The surface morphologies of GS0 and GS6 were visualized using field-emission scanning electron microscopy (SEM, Hitachi S-4800), operating at a typical accelerating voltage of 10 kV. Fourier transform

infrared spectra (FTIR) were obtained with a Bruker FTIR spectrometer (Bruker, Germany). The samples of GS0 and GS6 before and after adsorption of tetracycline were viewed with a glass slide on top of the quartz window of the ATR instrument. Measurements of micro Raman spectra were carried out using a Raman Scope system (LabRam-1B) with a 532 nm wavelength incident laser light and 20 mW power.

2.4. Batch sorption experiments

Batch experiments were conducted to evaluate the adsorption performance of tetracycline on the adsorbents. GS0 and GS6 were selected as adsorbents for tetracycline adsorption in an aqueous solution. 100 mg/L stock tetracycline solution was prepared by dissolving 100 mg tetracycline in 1 L deionized water. Working solutions of the required concentrations were obtained by diluting the stock solution with deionized water. All the sorption tests were conducted in well-capped 100 mL flasks containing 20 mL tetracycline solution with required concentration. After 10 mg of adsorbent was added, the flasks were shaken in a thermostatic shaker at 150 rpm at 298 K for 24 h. All the adsorption experiments were conducted in duplicate, and only the mean values were reported. The maximum deviation for the duplicates was usually <5%. The blank experiments without the addition of adsorbent were conducted to ensure that the decrease in the concentration was actually due to the adsorption rather than by the adsorption on the glass bottle wall. After adsorption, the adsorbent was separated by a 0.45 μm membrane. The residual concentrations in solution were determined by measuring absorbance changes at 364 nm. The adsorption isotherm was studied at pH 6 and the initial concentration solution was set from 1 to 50 mg/L. The adsorption capacity (mg/g) was calculated by following equation:

$$q_t = (C_0 - C_t) \times \frac{V}{m} \tag{1}$$

where C_0 and C_t are the initial concentrations and concentrations after a period of time (mg/L); V is the initial solution volume (L); and m is the adsorbent dosage (g).

The adsorption isotherm was calculated by Langmuir, Freundlich, Temkin, and Dubinin–Radushkevich (D–R) isotherms which were used to evaluate the adsorption equilibrium as in Eqs. (2)–(6). The Langmuir isotherm assumes that the adsorbate forms a monolayer around the homogenous surface of the adsorbent and that there is no interaction between the adsorbed molecules. The Freundlich model is an empirical one, which assumes that adsorption takes place on a heterogeneous surface and also proposes multilayer sorption with interaction among the adsorbed molecules.

The Temkin model is a proper model for the chemical adsorption based on strong electrostatic interaction between positive and negative charges. The D–R isotherm model does not assume a homogenous surface. Furthermore, the effect of the isotherm shape was studied to understand whether an adsorption system is favorable or not. Another important parameter, R_L, called the separation factor or equilibrium parameter, which can be used to determine the feasibility of adsorption in a given concentration range over adsorbent, was also evaluated by Eq. (7). The mean free energy of adsorption E_{DR} is related through Eq. (8) [14].

$$\frac{C_e}{q_e} = \frac{1}{K_L} + \left(\frac{\alpha_L}{K_L}\right) C_e \tag{2}$$

$$\ln q_e = \ln\ K_F + \frac{1}{n} \ln C_e \tag{3}$$

$$q_e = K_T \ln C_e + K_T \ln f \tag{4}$$

$$\ln q_e = \ln q_m - \beta \varepsilon^2 \tag{5}$$

$$\varepsilon_e = RT \ln\left(1 + \frac{1}{C_e}\right) \tag{6}$$

$$R_L = \frac{1}{1 + K_L C_0} \tag{7}$$

$$E_{DR} = \frac{1}{(2\beta)^{0.5}} \tag{8}$$

where K_L (L/g) and a_L (L/mg) are the Langmuir isotherm constants, respectively, and a_L relates to the energy of adsorption. When C_e/q_e is plotted against C_e, a straight line will be obtained. The value of K_L can be obtained from the intercept, which is $1/K_L$, and the value of a_L can be obtained from the slope, which is a_L/K_L. The maximum adsorption capacity of the adsorbent, $q_{m,cal}$, i.e. the equilibrium monolayer capacity or saturation capacity, is numerically equal to K_L/a_L; K_F, K_T are adsorption constants of Freundlich and Temkin models, respectively, and n is the Freundlich linearity index. The Langmuir model is an ideal model that has a perfect adsorbent surface and monolayer molecule adsorption. As an empirical model, the Freundlich model is used widely in the

field of chemistry. R (8.314 J/mol K) is the ideal gas constant and T (K) is the absolute temperature.

For a kinetic adsorption study, three common kinetic models (pseudo-first-order (9) that is based on solid capacity, pseudo-second-order (10) that is based on solid-phase adsorption, and intra-particle diffusion model (11) that describes the diffusion mechanism) were used to fit the experimental data and the correlation coefficient (R^2) was considered as a measurement of the agreement between the experimental data and the two proposed models [15].

$$\ln\,(q_e - q_t) = \ln q_e - \frac{k_1}{2.303}t \tag{9}$$

$$\frac{t}{q_t} = \frac{1}{k_2 q_e^2} + \frac{t}{q_e} \tag{10}$$

$$q_t = k_{id}\,t^{0.5} + C \tag{11}$$

where q_e and q_t are the amounts of tetracycline adsorbed (mg/g) at equilibrium and time t (h), respectively; k_1 is the rate constant of the pseudo-first-order kinetic model (t^{-1}); k_2 is the rate constant (g/mg h) of the pseudo-second-order kinetic model for adsorption; k_{id} (mg/g $h^{0.5}$) is the intra-particle diffusion rate constant, and C (mg/g) is the adsorption capacity calculated from this model.

The moisture content was calculated by Eq. (12).

$$\text{Moisture content } \% = \frac{m_e - m_0}{m_0} \tag{12}$$

where m_0 is the mass of aerogel and m_e is the mass of hydrogel.

3. Results and discussion

3.1. Influence of protein content on appearance

A digital camera image of GS0 and GS6 is shown in Fig. 1. It can be seen that the GS6 hydrogel is much looser than the GS0, which indicates that protein may keep the graphene from agglomeration. Moreover, it also can be seen that the GS0 hydrogel is floating, while the GS6 hydrogel stays in the bottom. There may be two reasons for their differences in structure and status in water. First, with a looser porous structure, the GS6 hydrogel could conserve more water. Second, the protein in the GS6 hydrogels also helped to absorb more water. The moisture content of hydrogels with different protein contents at room temperature are shown in Fig. 2.

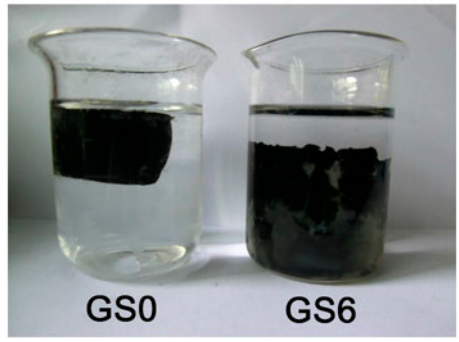

Fig. 1. Digital camera images of GS0 and GS6.

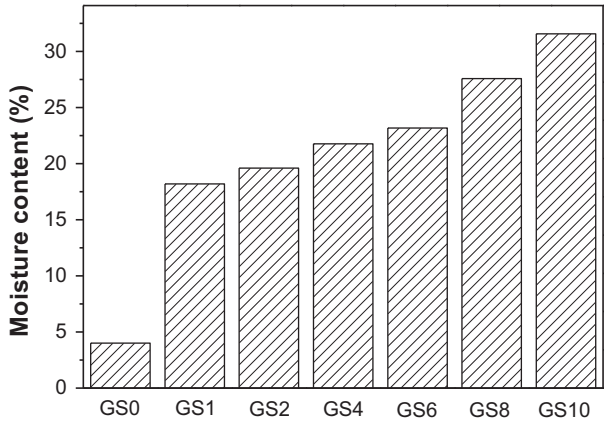

Fig. 2. Moisture content of GS hydrogels with different protein contents.

The moisture content increased significantly from 400 to 1,820% when the mass ratio of graphene to protein increased from 1:0 to 1:1, and the moisture content of GS10 reached 3,125%. This result further proved that the competition of hydrophilic protein interacted with water molecules much more strongly, which helped the composite hydrogels to contain more water.

3.2. Characterization of graphene and GS aerogel

SEM images of GS0 and GS6 are shown in Fig. 3(a) and (b). It can be seen that GS0 has a uniform surface, while the GS6 is rough. The figure also shows a rough and bulky surface, indicating pore interaction between the nanofillers and the matrix [16]. This result is because after composition, graphene was covered by protein. In addition, the protein separated the graphene from agglomeration. This linking mode has been reported as a "bricks" and "mortar" structure

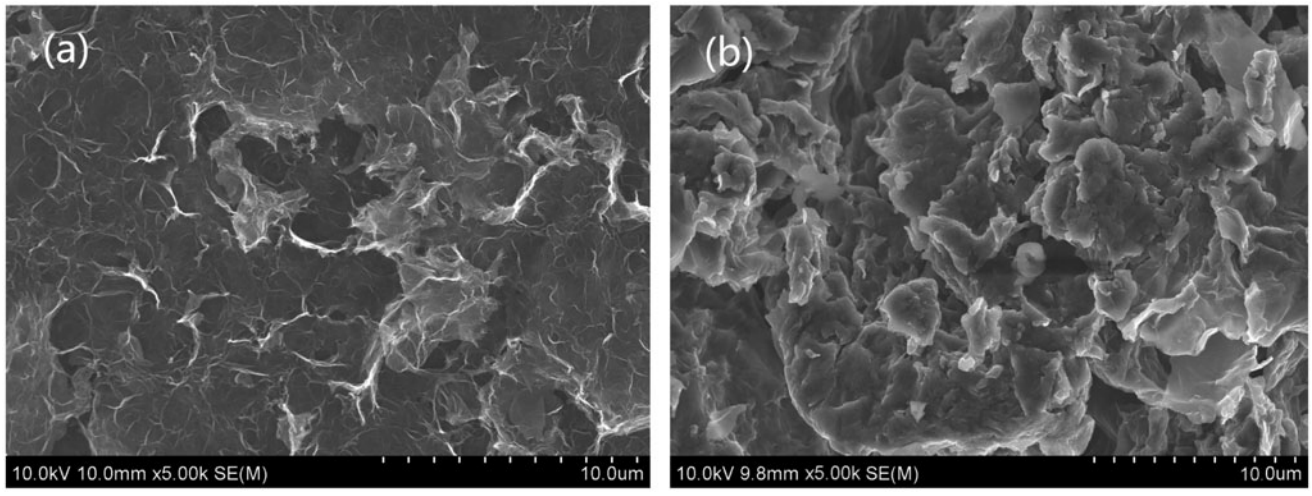

Fig. 3. SEM of GS0 (a) and GS6 (b) aerogels.

[17]; in this case, graphene and protein may also act as "bricks" and "mortar," respectively.

Raman spectroscopy of GS0 and GS6 is presented in Fig. 4. The presence of disorder in sp^2-hybridized carbon systems leads to rich and intriguing phenomena in their resonance Raman spectra; point defects are formed and the Raman spectra of the disordered graphene exhibit two new sharp features appearing at 1,345 and 1,626 cm^{-1}. These two features have, respectively, been called D and G bands, to denote disorder. All kinds of sp^2 carbon materials exhibit a strong Raman feature that appears in the range 2,500–2,800 cm^{-1} called the G′ band [18]. The G′ band, which is assigned as the distinct band of graphene induced by a two phonon resonant scattering process becomes broader after composition at 2,700 cm^{-1} indicates that GO was reduced to graphene [6]. The intensity ratios of the G band of graphene in the GS6 was weaker compared with that for GS0, further proving that protein isolated the graphene sheets.

3.3. Adsorption of tetracycline on aerogel with different protein contents

Tetracycline adsorptions on GS aerogels with different protein contents were investigated, as shown in Fig. 5. As is known that protein has little adsorption capacities and is much cheaper than graphene [19,20], we evaluated the adsorption capacities of the aerogels from two aspects: one is the common method used to calculate the adsorption capacity as in Eq. (1) and the other only uses the mass of graphene as the adsorbent dosage. We used the second one to select the best mass ratio of graphene to protein for a composite as

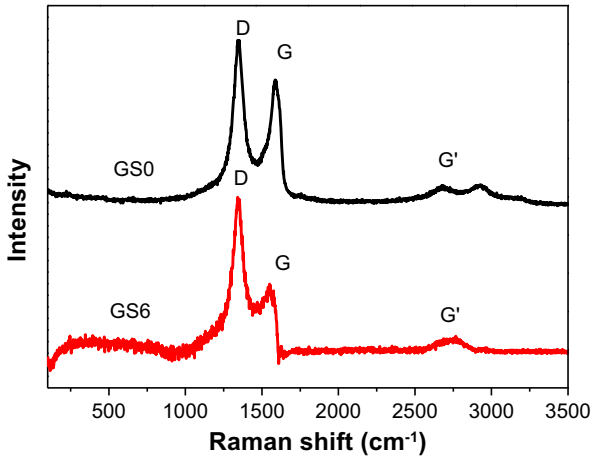

Fig. 4. Raman spectrum of GS0 and GS6.

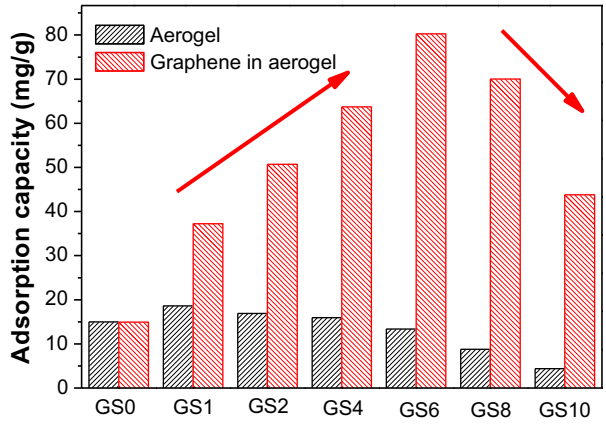

Fig. 5. Adsorption of tetracycline on GS hydrogels with different protein contents.

an adsorbent. Under the second calculation method, with the protein content rising, the adsorption capacity increased within a certain range and then decreased. The peak of adsorption capacity appeared in GS6, with an adsorption capacity of 80.26 mg/g. This result occurred because with the protein content rising, the composite has higher hydrophily and more functional groups that are beneficial for adsorption. However, the protein has fewer pores and has little adsorptivity. As a result, after protein content beyond certain range, the adsorption capacity of the composite decreased. Therefore, we used GS6 for the following characterization and adsorption comparison with the graphene aerogel.

3.4. Adsorption isotherms

The adsorption isotherm indicates the distribution relationship of the adsorbate molecules between the liquid phase and the solid phase when the adsorption process reaches equilibrium. The adsorption isotherm was calculated by Langmuir, Freundlich, Temkin, and D–R isotherm as shown in Fig. 6. The relative parameters calculated from the Langmuir and Freundlich models are listed in Table 1. Based on R^2 values, it can be seen from Table 1 that the adsorption isotherms are fitted well by both the Langmuir and the Freundlich models, followed by the Temkin and D–R isotherm models. It could be calculated from the Langmuir isotherm equation that the maximum theoretical adsorption capacity of tetracycline on GS6 was 164.0 mg/g, which was higher than graphene oxide-functionalized magnetic particles (39.1 mg/g) [4], modified bio-char (17.0 mg/g) [21]. The good regression coefficients of the Langmuir isotherm and the Temkin model present a good affinity between the tetracycline and aerogel. The values of R_L (0.019 for GS6 and 0.013 for GSO) between 0 and 1 indicate that

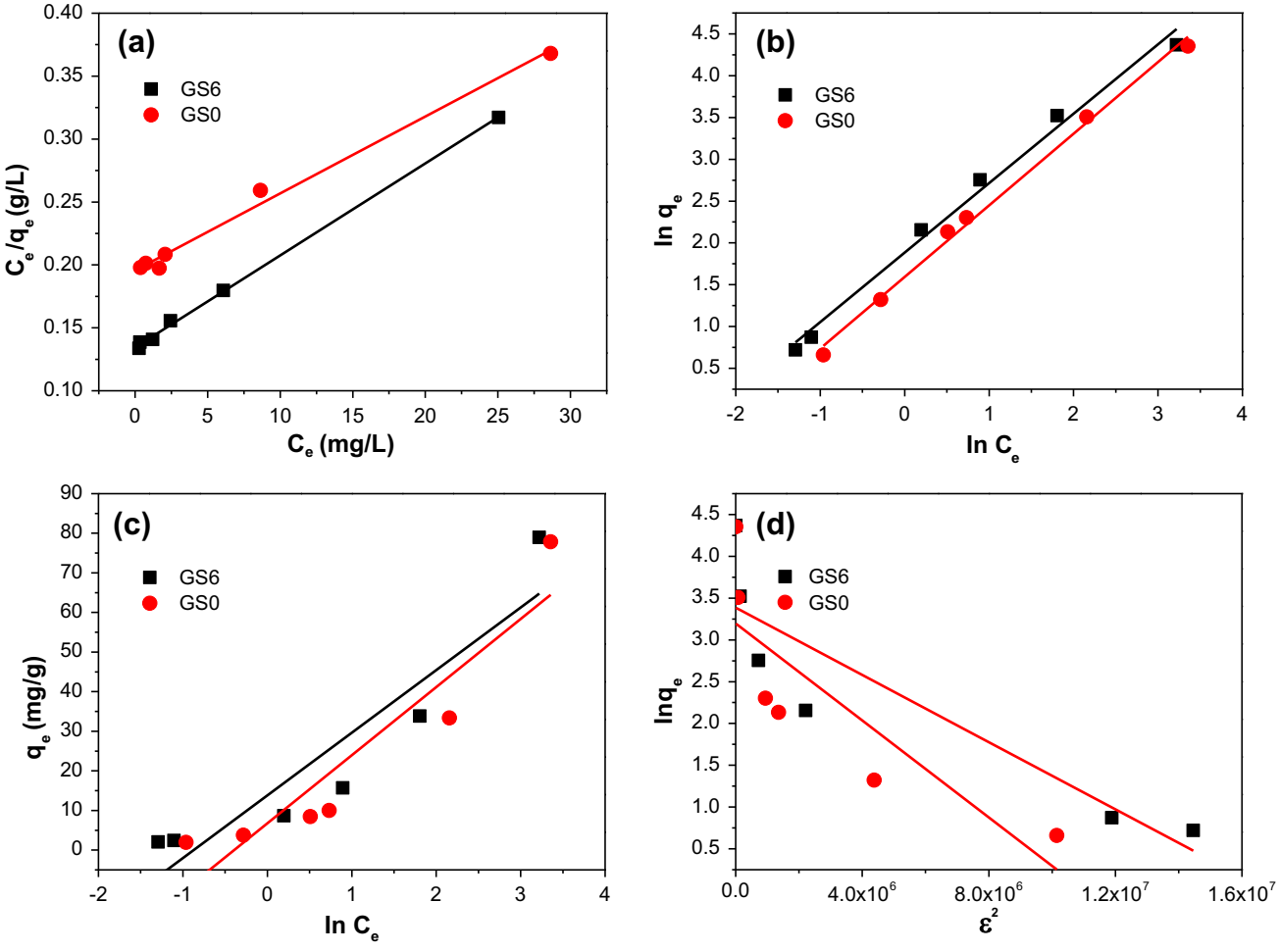

Fig. 6. Adsorption isotherm model of Langmuir (a), Frendlich (b), Tempkin (c), and D–R (d).

Table 1
The parameters derived from the Langmuir, Freundlich, Temkin, and D–R models

Isotherm	Characteristic	GS6	GS0
Langmuir	q_m (mg/g)	164.0	137.0
	K_L	5.110	7.440
	R^2	0.990	0.999
Freundlich	K_F	6.580	4.914
	n	1.205	1.168
	R^2	0.988	0.994
Temkin	K_T	15.816	17.193
	R^2	0.827	0.835
D–R	q_m (mg/g)	29.5	24.5
	β (mol^2/kJ^2)	2.901	2.011
	E (kJ/mol)	2.409	2.005
	R^2	0.622	0.770

the adsorption is favorable. Moreover, the n values for the Freundlich isotherm are between 1 and 10 (1.205 for GS6 and 1.168 for GS0), further proving that the adsorption is favorable under the studied conditions.

3.5. Adsorption kinetics

A change of adsorption capacity over time is shown in Fig. 7(a), where it can be seen that the adsorption capacity increases quickly in the first 10 h, slowly increases thereafter, and reaches equilibrium around 24 h. The adsorption data were fitted by the pseudo-first-order, the pseudo-second-order, and the intra-particle diffusion model, as shown in Fig. 6. The parameters are presented in Table 2. The pseudo-first-order model provided the best fitting for all the experimental data. The plots showed high regression coefficients ($R^2 = 0.993$). The k_1 value was 0.002 min^{-1}, indicating a moderate speed of adsorption. Also, the q_e

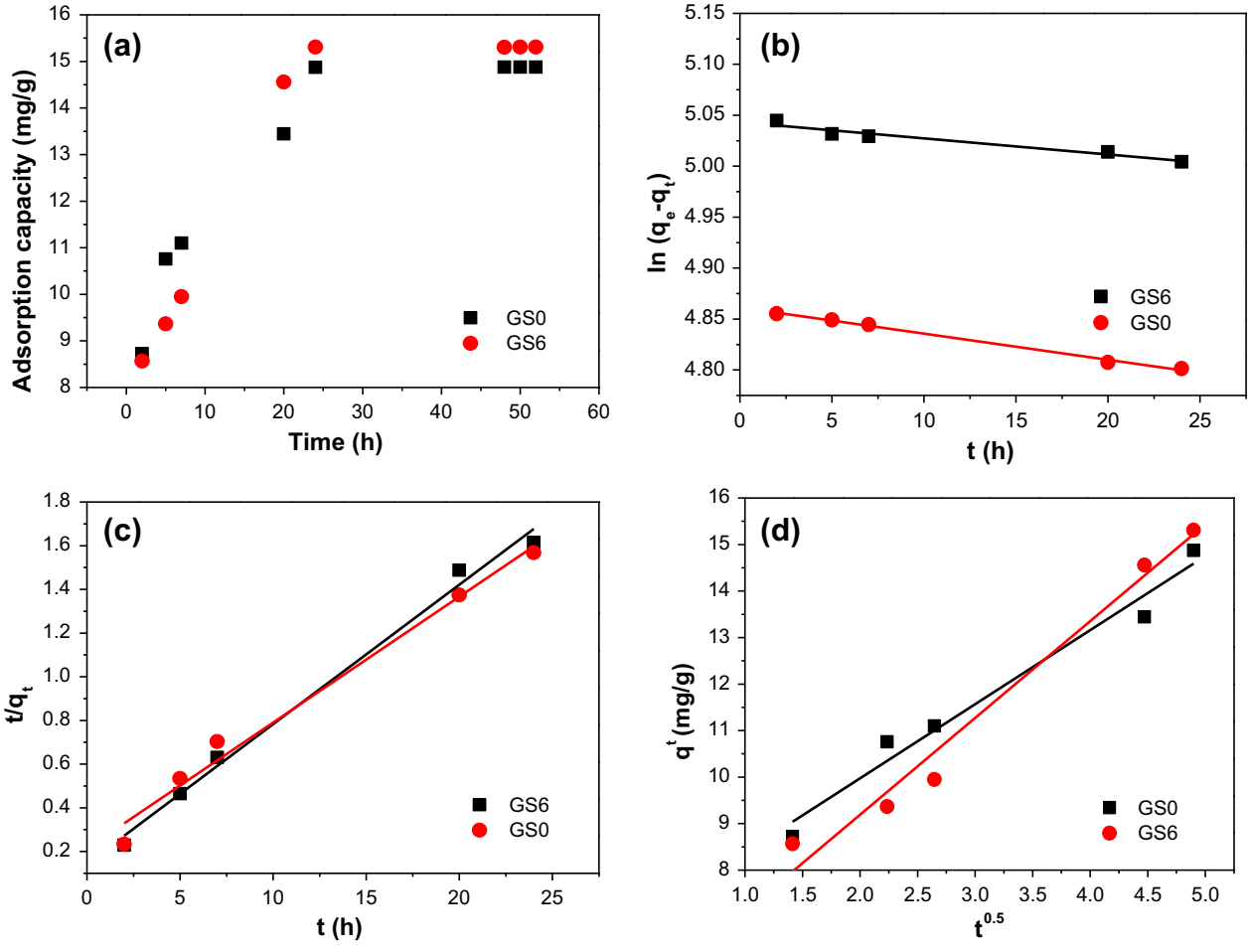

Fig. 7. Kinetic curves (a), kinetics analyses of pseudo-first-order model (b), pseudo-second-order model (c), and intra-particle diffusion model (d).

Table 2
Kinetic parameters of pseudo-first- and pseudo-second-order adsorption kinetic models and intra-particle diffusion model on GS0 and GS6

	Pseudo-first-order			Pseudo-second-order			Intra-particle diffusion		
Adsorbent	q_e (mg/g)	k_1 (min^{-1})	R^2	q_e (mg/g)	k_2 (min^{-1})	R^2	k_{id} (mg/g $min^{0.5}$)	C (mg/g)	R^2
GS6	155.0	0.002	0.993	15.6	0.028	0.981	1.592	6.790	0.967
GS0	129.2	0.004	0.994	17.4	0.016	0.990	2.080	5.031	0.971

values obtained by the pseudo-first-order equation are 155.0 mg/g (GS6) and 129.2 mg/g (GS0), which are close to the values obtained by the Langmuir model. The q_e values obtained by the pseudo-second-order equation are 15.6 mg/g (GS6) and 17.4 mg/g (GS0), which are close to the values obtained by the experiment, indicating that the adsorption follows the pseudo-second-order kinetics better. Fig. 7(d) shows that the graph is not completely linear and does not pass through the origin of the coordinate, suggesting that there are other kinetic factors that control the adsorption rate apart from intra-particle diffusion.

3.6. Influence of pH on adsorption

The influence of pH on adsorption is shown in Fig. 8. Tetracycline is an amphoteric molecule with multiple ionizable functional groups: a tricarbonylamide group, a phenolic diketone group, and a dimethyl amino group. Tetracycline can undergo protonation–deprotonation reactions and present different species depending on the solution pH. Dissolved tetracycline species may have net charges that are positive (H_3TC^+, pH < 3.3), neutral (H_2TC°, 3.3 < pH < 7.68), one negative (HTC^-, 7.68 < pH < 9.68), or two negative (TC^{2-}, pH > 9.68) [22]. It can be seen from Fig. 4 that the adsorption of tetracycline on the aerogel was pH-dependent. The GS0 showed better adsorption capacity under an alkaline solution, while the GS6 was better under a neutral solution; both aerogels showed a lower adsorption capacity under acid circumstances. This result might be attributed to the molecular structure of tetracycline and the functional groups present on the surface of the aerogel. Possibly, the deprotonation of carboxyl groups of the aerogel was enhanced under alkaline conditions, which strengthened the electrostatic interaction with amino groups on tetracycline [10]. Moreover, the variation in pH not only focuses on the protonation–deprotonating transition of functional groups, but also results in a change in chemical speciation [23].

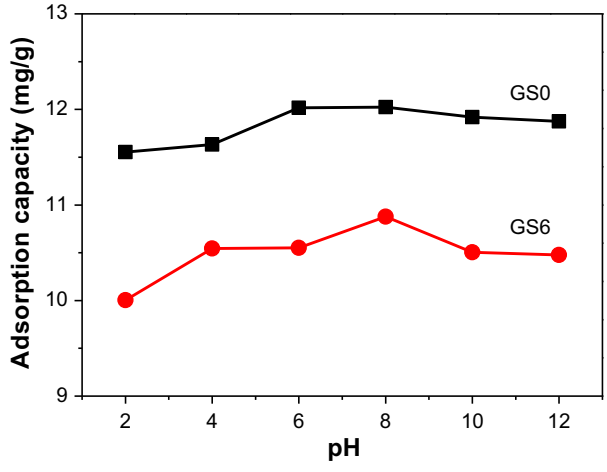

Fig. 8. Influence of pH on tetracycline adsorption on GS0 and GS6.

3.7. FTIR analysis of aerogel before and after adsorption

Before and after adsorption, GS0 and GS6 are analyzed by FTIR, as shown in Fig. 9(a) and (b). Before adsorption, GS6 contains many more functional groups than GS0. Amide I (due to the high C=O group extinction coefficient) and NH_2 bands at 1,647 and 1,590 cm^{-1} appeared in GS6 rather than in GS0; the band at around 3,100 cm^{-1} in GS6 should be assigned to O–H, as well as to intermolecular hydrogen bonding within the aerogel; it further accounts for the excellent hydrophily of GS6 [24]. Methylene (CH_2) asymmetric and symmetric modes are at 2,875 and 2,855 cm^{-1}; after adsorption, peaks around 2,240 cm^{-1} appeared in both GS0 and GS6, which indicated that graphene and tetracycline formed C ≡ C after adsorption. Moreover, functional groups in GS6 apparently decreased after adsorption, indicating that the chemical reaction played an important role in this adsorption. The benzene rings can act as a π-electron-acceptor while the –OH groups on the graphene surface can make the graphene act as electron donors. Thus, significant enhanced sorption was expected by the formation of a π–π bond.

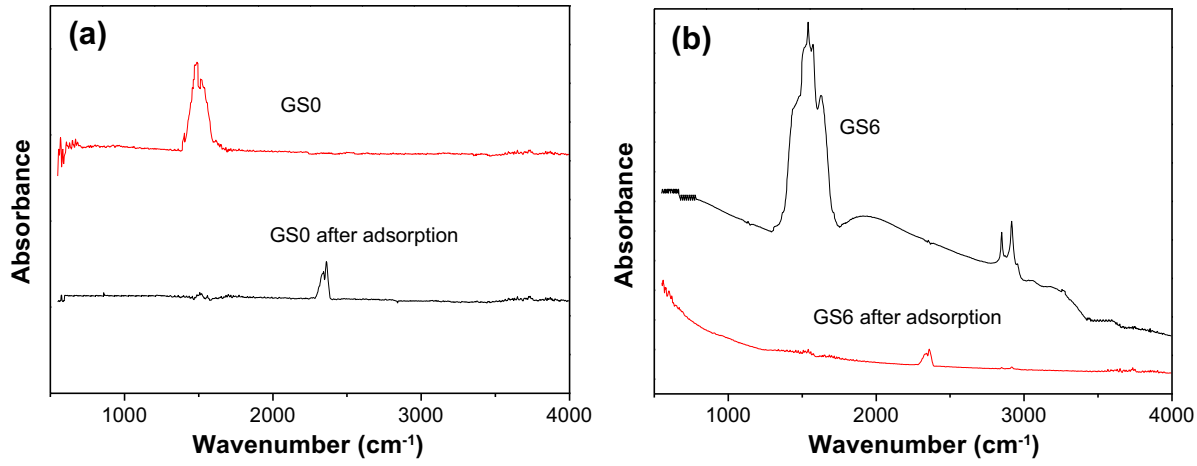

Fig. 9. FTIR analysis of GS0 (a) and GS6 (b) aerogels before/after adsorption.

4. Conclusion

A 3D graphene–soy protein composite aerogel was prepared and used in tetracycline adsorption. The composite hydrogels GS6 have a looser structure, better hydrophobicity, and more functional groups than graphene hydrogel GS0. The protein in the composite appeared to cover the graphene in micro-structure, and Raman analysis further proved that graphene turned out to be separated by protein, which prevents it from aggregation. The adsorption capacity of the aerogels relatively increased with the protein content rising in certain contexts. Both the physical and the chemical adsorptions take effect in this adsorption. Calculated from the Langmuir model, the maximum adsorption capacity of GS0 was 137.0 mg/g, while GS6 was 163.934 mg/g. The Langmuir and the pseudo-second-order were best fitted for both GS0 and GS6. As protein has little adsorption potent itself but is cheap and nontoxic, the graphene–soy protein composite aerogel has marked improvement for its use as adsorbent or biological applications.

References

[1] J.G. da Silva, M.A. Hyppolito, J.A. de Oliveira, A.P. Corrado, I.Y. Ito, I. Carvalho, Aminoglycoside antibiotic derivatives: Preparation and evaluation of toxicity on cochlea and vestibular tissues and antimicrobial activity, Bioorg. Med. Chem. 15 (2007) 3624–3634.
[2] M. Peterson, Hyperthyroidism in cats: What's causing this epidemic of thyroid disease and can we prevent it? J. Feline Med. Surg. 14 (2012) 804–818.
[3] L. Ji, W. Chen, L. Duan, D. Zhu, Mechanisms for strong adsorption of tetracycline to carbon nanotubes A comparative study using activated carbon and graphite as adsorbents, Environ. Sci. Technol. 43 (2009) 2322–2327.
[4] Y. Lin, S. Xu, J. Li, Fast and highly efficient tetracyclines removal from environmental waters by graphene oxide functionalized magnetic particles, Chem. Eng. J. 225 (2013) 679–685.
[5] H. Chen, B. Gao, H. Li, Functionalization, pH, and ionic strength influenced sorption of sulfamethoxazole on graphene, J. Environ. Chem. Eng. 2 (2014) 310–315.
[6] J.N. Tiwari, K. Mahesh, N.H. Le, K.C. Kemp, R. Timilsina, R.N. Tiwari, K.S. Kim, Reduced graphene oxide-based hydrogels for the efficient capture of dye pollutants from aqueous solutions, Carbon 56 (2013) 173–182.
[7] V. Georgakilas, M. Otyepka, A.B. Bourlinos, V. Chandra, N. Kim, K.C. Kemp, P. Hobza, R. Zboril, K.S. Kim, Functionalization of graphene: Covalent and non-covalent approaches, derivatives and applications, Chem. Rev. 112 (2012) 6156–6214.
[8] Z. Zhao, X. Wang, J. Qiu, J. Lin, D. Xu, C.A. Zhang, M. Lv, X. Yang, Three-dimensional graphene-based hydrogel/aerogel materials, Rev. Adv. Mater. Sci. 36 (2014) 137–151.
[9] C.S. Cheng, J. Deng, B. Lei, A. He, X. Zhang, L. Ma, S. Li, C. Zhao, Toward 3D graphene oxide gels based adsorbents for high-efficient water treatment via the promotion of biopolymers, J. Hazard. Mater. 263 (Pt 2) (2013) 467–478.
[10] L. Zhao, P. Dong, J. Xie, J. Li, L. Wu, S.-T. Yang, J. Luo, Porous graphene oxide–chitosan aerogel for tetracycline removal, Mater. Res. Express. 1 (2013) 015601-1–015601-11.
[11] Y. Xu, Q. Wu, Y. Sun, H. Bai, G. Shi, Three-dimensional self-assembly of graphene oxide and DNA into multifunctional hydrogels, ACS Nano 4 (2010) 7358–7362.
[12] K. Nishinari, Y. Fang, S. Guo, G.O. Phillips, Soy proteins: A review on composition, aggregation and emulsification, Food Hydrocolloids 39 (2014) 301–318.
[13] W.S. Hummers, R.E. Offeman, Preparation of graphitic oxide, J. Am. Chem. Soc. 80 (1958) 1339–1340.
[14] X. Wang, R. Sun, C. Wang, pH dependence and thermodynamics of Hg(II) adsorption onto chitosan-poly(vinyl alcohol) hydrogel adsorbent, Colloids Surf., A 441 (2014) 51–58.

[15] G. Zhao, J. Li, X. Wang, Kinetic and thermodynamic study of 1-naphthol adsorption from aqueous solution to sulfonated graphene nanosheets, Chem. Eng. J. 173 (2011) 185–190.
[16] C. Rodríguez-González, A.L. Martínez-Hernández, V.M. Castaño, O.V. Kharissova, R.S. Ruoff, C. Velasco-Santos, Polysaccharide nanocomposites reinforced with graphene oxide and keratin-grafted graphene oxide, Ind. Eng. Chem. Res. 51 (2012) 3619–3629.
[17] L. Huang, C. Li, W. Yuan, G. Shi, Strong composite films with layered structures prepared by casting silk fibroin-graphene oxide hydrogels, Nanoscale 5 (2013) 3780–3786.
[18] M.S. Dresselhaus, A. Jorio, M. Hofmann, G. Dresselhaus, R. Saito, Perspectives on carbon nanotubes and graphene Raman spectroscopy, Nano Lett. 10 (2010) 751–758.
[19] P. Kar, M. Misra, Use of keratin fiber for separation of heavy metals from water, J. Chem. Technol. Biotechnol. 79 (2004) 1313–1319.
[20] S. Wang, H. Sun, H.M. Ang, M.O. Tadé, Adsorptive remediation of environmental pollutants using novel graphene-based nanomaterials, Chem. Eng. J. 226 (2013) 336–347.
[21] P. Liu, W.J. Liu, H. Jiang, J.J. Chen, W.W. Li, H.Q. Yu, Modification of bio-char derived from fast pyrolysis of biomass and its application in removal of tetracycline from aqueous solution, Bioresour. Technol. 121 (2012) 235–240.
[22] Y. Zhao, F. Tong, X. Gu, C. Gu, X. Wang, Y. Zhang, Insights into tetracycline adsorption onto goethite: Experiments and modeling, Sci. Total Environ. 470–471 (2014) 19–25.
[23] E.E. Ghadim, F. Manouchehri, G. Soleimani, H. Hosseini, S. Kimiagar, S. Nafisi, Adsorption properties of tetracycline onto graphene oxide: Equilibrium, kinetic and thermodynamic studies, PLOS ONE 8 (2013) e79254-1–e79254-9.
[24] A.L. Caroni, C.R. de Lima, M.R. Pereira, J.L. Fonseca, Tetracycline adsorption on chitosan: A mechanistic description based on mass uptake and zeta potential measurements, Colloids Surf., B 100 (2012) 222–228.